J. COMBIN. MATH. COMBIN. COMPUT. 127b (2025) 6473--6498

Journal of Combinatorial Mathematics and Combinatorial Computing
www.combinatorialpress.com/jcmcc

Collaborative Research on Panoramic Display of Grid One Map Production Information and Big Data Analysis Algorithm Based on Electricity 3D Engine

Lingxu Guo[1,2,✉], Shiqian Ma[2], Yifang Li[3], Ping Tang[2], Shengyuan Gao[3], Wanle Ma[3]

[1] *Department of Electrical Engineering, Tsinghua University, Beijing, 100084, China*

[2] *State Grid Tianjin Electric Power Company, Tianjin, 300010, China*

[3] *Beijing Yongshang Technology Co., Ltd, Beijing, 100085, China*

ABSTRACT
The power grid, as a unified whole composed of various links of generation, transmission, transformation, distribution and use, needs mutual coordination and unified scheduling in terms of operation characteristics. This paper establishes a power 3D engine based on lightweight 3D engine technology, and builds a panoramic display platform for grid one map generation information on this basis. In order to explore the feasibility of this platform on grid optimization and scheduling, this paper establishes a two-layer optimization and scheduling model of the grid by taking the minimization of the operation cost as the objective function of the upper layer, and combining the supply-side and demand-side balancing objectives of the lower microgrid. The PSO algorithm is improved by introducing the immune mechanism, linear adjustment, and linear combination, and the HPSO algorithm is used to solve the grid two-layer optimal dispatch model. The simulation shows that the economic cost and environmental cost are reduced by 51.78% and 23.07%, respectively, and the total cost is reduced by 8.66*106 yuan after considering the uncontrollable residential electricity load. Relying on the One Grid Map platform can realize the accurate analysis of the peaking capacity and climbing residual capacity of the grid at typical time periods, providing reliable data support to meet the peak shaving and valley filling of the grid. Combined with the lightweight 3D engine technology, the panoramic display platform of production information of one map of power grid helps to obtain real-time grid operation and environmental information, realize monitoring and comprehensive analysis of the system, and make real-time decisions and interactions for optimal dispatching of power grid.

Keywords: one map of power grid, lightweight 3D engine, power 3D engine, grid optimization scheduling, HPSO algorithm

✉ Corresponding author.
E-mail address: lingxuguo@outlook.com (L. Guo).
Received 20 February 2024; Revised 25 April 2024; Accepted 20 November 2024; Published Online 16 April 2025.
DOI: 10.61091/jcmcc127b-355

1. Introduction

Driven by the wave of digitization, the power industry is undergoing unprecedented changes. As one of the core technologies of this change, "One Grid Map" has not only reshaped the face of power grid management, but also revolutionized power marketing management. Grid one map system is the generation, transmission, substation, distribution, electricity and other aspects of real-time data, equipment status and operational information through digital means integrated in a map. It covers the detailed data of grid equipment of all voltage levels from high voltage to low voltage, including substations, transmission lines, distribution lines and low voltage platforms, etc., realizing the digital management of all elements of the grid [1-2]. It also provides richer information resources for marketing management by real-time aggregation of static and dynamic information of the grid itself, as well as multi-dimensional data such as meteorological environment and video surveillance [3-4]. In addition, as a graphical service platform for cross-disciplinary integration of applications, "One Grid Map" provides an intuitive and convenient operation interface for marketing management and supports the lightweight construction of enterprise-level application scenarios [5-7]. It can be seen that the grid one map system is an important carrier for grid enterprises in the process of digital construction and transformation.

In the construction and application field of intelligent electric field, 3D modeling plays an important role in digital design, digital handover, intelligent construction site, intelligent monitoring, intelligent security, and intelligent inspection [8-9]. For personnel positioning, SIS, and smart construction sites, 3D modeling can provide scene support and correlate real-time data with 3D models [10]. For systems such as intelligent monitor, video linkage, personnel positioning, etc., it can be directly involved in data processing and enhance the data processing capability of the original system [11]. In the construction of intelligent power system, to let the three-dimensional model carry more data, it is necessary to associate each model with the data source, and thus the introduction of intelligent algorithms to improve the efficiency of the three-dimensional engine is of great significance [12-14].

The scale of the regional power grid is expanding, the operation mode is also becoming more and more complex, the connection and coupling degree between transmission and distribution networks is becoming more and more close, the existing transmission and distribution network automation system independent operation mode can not fully adapt to the future power grid operation, management, scheduling and other business development requirements. The article will be the physical entities of the power grid, abstract entities for simplification, combined with hierarchical resource management and greedy strategy dynamic scheduling, the introduction of power grid cascade lightweight loading, so as to build the power three-dimensional engine. Based on the architecture of power 3D engine, a panoramic display platform for production information of one map of power grid is designed. For the optimal scheduling performance of the one-grid map, a two-layer optimal scheduling model of the grid is designed based on the consideration of minimizing the operation cost and the supply side and demand side of the microgrid. Various improvement mechanisms are introduced to optimize the traditional PSO algorithm, and the improved PSO algorithm is used to solve the two-layer optimal scheduling model. Data analysis is carried out for its simulation results, and the specific performance of the grid one map platform is tested.

2. Grid a map production information panoramic platform

The One Grid Map platform integrates the real-time data, equipment status and operation information of power generation, transmission, substation, power distribution, power consumption and other links on one map by digital means, and its static grid map based on the basic data of the grid resource business center is superimposed on the dynamic data of the real-time measurement center to form a dynamic grid map. The basic data of one map of power grid is maintained by the same source system, which is an important carrier for power grid enterprises in the process of digital construction and transformation.

2.1. Lightweight engine key technology

2.1.1. Streamlining of physical and abstract entities:

1) Physical Entity Streamlining. Streamlining of physical entities, such as substations, significantly reduces the data volume of the model while maintaining visual quality through surface reduction compression and texture optimization. Reduced surface compression reduces the overall complexity of the model by reducing redundant parts in the model structure, thus realizing a reduction in the model volume. Network model simplification (QEM) is a widely used facet reduction algorithm that utilizes the quadratic error matrix of the vertices to evaluate the impact of merging vertices on the model. To wit:

$$Q(v_i) = \sum_{k=1}^{3} (a_k v_i^k + b_k)^2 + c_k \tag{1}$$

Where $Q(v_i)$ is the quadratic error matrix associated with the vertices v_i, and a_k, b_k, and c_k are coefficients associated with the geometric attributes of the model Reduced Surface The goal of the surface reduction is to minimize the total error while reducing the number of polygons.

Texture data usually occupies most of the space in a 3D model file, and texture compression techniques are an effective way to reduce the size of the model file and improve the loading performance. Texture compression can be described by the following equation:

$$C(T) = \frac{\sum_{i=1}^{u} \left| T_i - T_i' \right|^L}{n} \tag{2}$$

T is the original texture image, T' is the compressed texture image, n is the total number of pixels, and $C(T)$ is the compression error. The goal of texture optimization is to reduce the size of the texture data while minimizing the compression error $C(T)$.

2) Abstract entity streamlining. For abstract entity rendering for lines, extreme weather paths, etc., the 3D engine adopts the curve thinning algorithm to sample its nodes and lines to reduce the complexity of the line model and keep the key features of the lines as much as possible. Define the objective function f, while considering the approximation error of the curve and the complexity of the curve:

$$f(L') = \alpha \cdot Error(L, L') + \beta \cdot Complexity(L') \tag{3}$$

Where L is the original grid line curve, L' is the simplified curve, and α and β are weight parameters to balance error and complexity. $Error(L, L')$ measures the difference between L and L', while $Complexity(L')$ quantifies the complexity of the simplified curve.

To find the optimal simplified curve L', a heuristic search strategy is used to randomly select a simplified point set S starting from the original curve L. For each point p in the point set S, calculate the objective function $f(L')$ of the curve L' after removing p. Select the point p that minimizes $f(L')$ for removal and update the simplified point set S. The iteration is stopped when a predetermined number of iterations is satisfied or the improvement of $f(L')$ is below a certain threshold. By evaluating and selecting the best simplification path at each iteration step, the complexity of the model is significantly reduced while maintaining the critical characteristics of the grid line curve.

3) Abstract concept streamlining. For the streamlined presentation of abstract concepts such as voltage, oscillations, and faults, taking bus voltage as an example, Radial Basis Function (RBF) interpolation is used to generate continuous voltage levels between data points, and for each data point (x_i, y_i), its distance $r_{i,j}$ from each point (x, y) on the grid is calculated. The weights $\phi(r_{i,j})$ are then calculated using RBF. Construct the linear system $Ax = V$, where the elements $a_{i,j}$ of the

matrix A are determined by $\phi(r_{i,j})$, x is the vector of unknown coefficients, and V is the vector of known voltage values. Solve the linear system $Ax=V$ using numerical methods to obtain the coefficient vector x. For any point (x,y) on the grid, interpolate using the following equation, i.e.:

$$V(x,y)=\sum_{i=1}^{n} x_i\cdot\phi(\sqrt{(x-x_i)^2+(y-y_i)^2}) \tag{4}$$

Where $V(x,y)$ is the voltage at the interpolated point and n is the number of data points, the voltage contour plot is drawn from the interpolation results using a plotting software or library. The interactive experience can be enhanced by streamlining the presentation of abstract concepts with which the user can interact in the meta-universe. Examples include adjusting voltage levels, observing the effects of oscillations, or simulating fault conditions to gain a deeper understanding.

2.1.2. Resource management and dynamic scheduling:

1) Hierarchical Resource Management. The core idea of the main resource fairness algorithm (DRF) is to calculate the main resources and main shares of each subtask based on the resource demand vectors of different subtasks of the user and the resource vectors that can be allocated by the cluster, and then get the final fair allocation scheme by balancing the main shares. In the Grid-a-Map platform, suppose there exist two resource types r_1 and r_2 (e.g., CPU and memory), and the corresponding total amount of resources are R_1 and R_2, respectively. If the demand vector of subtask i submitted by user I is $D_i=<d_{ir1},d_{i,r2}>$, and the demand vector of subtask j submitted by user II is $D_j=<d_{jr1},d_{j,r2}>$, then the corresponding main shares of users I and II are \$ S_i and S_j are respectively:

$$S_i=x_i\times\max(\frac{d_{i,r1}}{R_1},\frac{d_{i,r2}}{R_2}) \tag{5}$$

$$S_j=x_j\times\max(\frac{d_{j,r1}}{R_1},\frac{d_{j,r2}}{R_2}) \tag{6}$$

and the following constraints need to be satisfied:

$$\begin{cases} d_{i,r1}x_i+d_{j,r1}x_j\le R_1 \\ d_{i,r2}x_i+d_{j,r2}x_j\le R_2 \\ S_i=S_j \end{cases} \tag{7}$$

where x_i and x_j denote the number of subtasks i and j in the fair allocation of cluster resources.

2) Dynamic Scheduling with Greedy Policy. Consider a dynamic task scheduling scenario, where the task queue and resource status are monitored in real time and scheduling decisions are made quickly. The greedy policy is used to identify the current set of tasks to be scheduled and their resource requirements, evaluate the current available resource status, formulate resource allocation decisions based on the current task and resource status, and execute them, collect the execution results as feedback to realize the local optimal choice.

It is assumed that the resource requirements and system resource state of task T can be described in detail by the following parameters. $C(T)$ denotes the computational resource requirement of task T, $S(T)$ denotes the storage resource requirement of task T, $N(T)$ denotes the network resource requirement of task T, $P(T)$ denotes the projected execution time of task T, $D(T)$ denotes the deadline urgency of task T, and $R(T)$ denotes the historical utilization of resources of task T. The utility function $U(T)$ can be defined as:

$$U(T)=(\frac{\omega_C C(T)}{C_{\max}}+\frac{\omega_S S(T)}{S_{\max}}+\frac{\omega_N N(T)}{N_{\max}})\cdot(\frac{1}{P(T)})^{\alpha}\cdot(\frac{D(T)}{P(T)})^{\beta}\cdot(1-e^{-\gamma\cdot K(T)}) \tag{8}$$

where $C_{\max}, S_{\max}, N_{\max}$ are the maximum computational, storage, and network resources available to the system, respectively, α and β are the weight factors that adjust the urgency of the task execution times and deadlines, and γ is a weight factor that adjusts the impact of the historical utilization of resource weight factor of resource scheduling strategy. $\frac{1}{P(T)}$ denotes the inverse of the task execution time and encourages priority scheduling of tasks with short execution times, $\frac{D(T)}{P(T)}$ denotes the relative deadline urgency of the task and encourages priority scheduling of tasks with close deadlines, and $e^{-\gamma\cdot R(T)}$ is an attenuating factor to reduce the priority of tasks that overuse resources. At each resource allocation decision, the algorithm evaluates the utility function $U(T)$ of all tasks to be allocated and selects the task with the largest $U(T)$ value for resource allocation.

2.1.3. Lightweight loading of power grid cascades. In the process of establishing the 3D model of the power grid, 3D modeling technology is used to analyze the structure of the original power grid model and optimize the 3D model of the power grid. It is set that there are 2 types of objects in the grid model, and the different connection points in the grid are represented as nodes D. All nodes are connected and their physical paths are represented as lines K. The relationship between the 2 types of objects is described by applying mathematical formulas, and the model is:

$$F=\frac{D_i}{K_{ij}} \tag{9}$$

where D_i is the set of nodes directly connected to node i and i, j are nodes. By analyzing different objects in the model, it is possible to fully parse the grid structure, obtain the relationship between different objects, and simulate the behavior of the objects under different conditions in the grid.

By combining the chunk indexing with the LOD technique, the model is divided into multiple LOD levels and the model that matches its level is used at different distances. During the division process, the quadtree method is applied to quadrant the space within the scene to quickly exclude the parts that are unlikely to contain the model and reduce unnecessary rendering. The simplified model is used as the root node to determine the appropriate node rendering resolution when the 3D model of the grid is loaded in real time, and the scheduling efficiency is improved by controlling the amount of model loaded.

Set the quadtree node in the scene as $g(x)$, and T is the actual number of rendered models. Its scheduling formula is:

$$T=\sum_{i}^{n-1} g(x)+n_i \tag{10}$$

where n_i is the ith quadtree node that intersects and $g(x)$ is the total number of quadtree nodes. Starting from the root node, check whether the grid 3D model intersects with the quadtree nodes. When there is no intersection, this node and all its children are ignored. If an intersection exists, all nodes need to be rechecked and their associated children ranked until a leaf node is reached or it is determined that the node does not need to be rendered. For each leaf node that needs to be rendered, its corresponding model is loaded and rendered. To render the model more realistically, render the outline of the model when the node is far from the viewpoint. When the nodes are close to the viewpoint, high resolution is used to show the subtle features of the terrain in order to provide a more realistic visualization. Therefore, the establishment of the rendering resolution function, by controlling the function within the range of the rendering threshold, can ensure the realization of efficient and realistic terrain rendering in different situations. Its fulfillment condition is:

$$f(z) = \frac{\max(\beta \frac{\Delta d}{t})}{m} < B \tag{11}$$

where β is a constant, B is the control threshold of rendering resolution, and m is the edge length of the model chunks.

The data chunks of different levels are added to the memory by CPU in real time, and the multidimensional matrix processing of the quadtree model is performed by GPU stream processing technology, and the corresponding vertices are smoothed to solve the anomalies appearing in the model rendering. The vertex data in different chunks are transferred to the shader to realize the rendering of the 3D model of the power grid in order to reduce the amount of data transfer between the memory and the video memory to a certain extent, so as to improve the efficiency of rendering the 3D model of the power grid.

2.2. Power 3D engine construction

2.2.1. Lightweight 3D engine construction principles. Lightweight Technology explores the principles of lightweight design under model volume and innovative methods to reduce resource consumption. The design and construction of the lightweight 3D engine aims to provide an advanced lightweight engine to enhance the information expression and interaction effectiveness of power dispatching. The grid 3D engine integrates geographic terrain information and complex topological models of the power system, massive high-frequency real-time data, and applies real-time 3D engine technology to achieve the visualization of the grid structure, real-time analysis of power data, real-time reach of grid operation, and the underlying support of the grid's internal communication with high timeliness and low latency.

Therefore, in terms of 3D engine construction, reasonable resource management and dynamic scheduling techniques are considered for equipment and element modeling, generating highly detailed 3D models to enhance the running speed of the lightweight engine. In terms of supporting geo-navigation of external operation data, the integration of power grid model with geographic information, meteorological environment, and operation information is considered in order to realize comprehensive monitoring and early warning of power dispatch meta-universe application scenarios. The lightweight 3D engine shapes the data-driven real-time dynamic power grid digital space model by building powerful graphic processing and rendering capabilities, presents various power dispatching business scenarios in a multi-dimensional 3D visualization style, monitors power grid operation in real time, and quickly generates reports and responses.

2.2.2. Power Light 3D Engine Architecture. The power dispatch meta-universe supported by lightweight 3D engine is constructed to realize the efficient expression of geographic information, high-frequency meteorology, power grid model information, and real-time information. The design architecture of the lightweight 3D engine for power dispatching is shown in Figure 1. The lightweight 3D engine of power dispatching meta-universe takes data as the underlying foundation, builds the corresponding dynamic and static models in the meta-universe scene on the basis of the data, and carries out the rapid rendering of the scene and objects, relies on the data to build the logical reasoning ability of the engine, and is assisted by the corresponding lightweight technical means to improve the performance of the engine in different working environments.

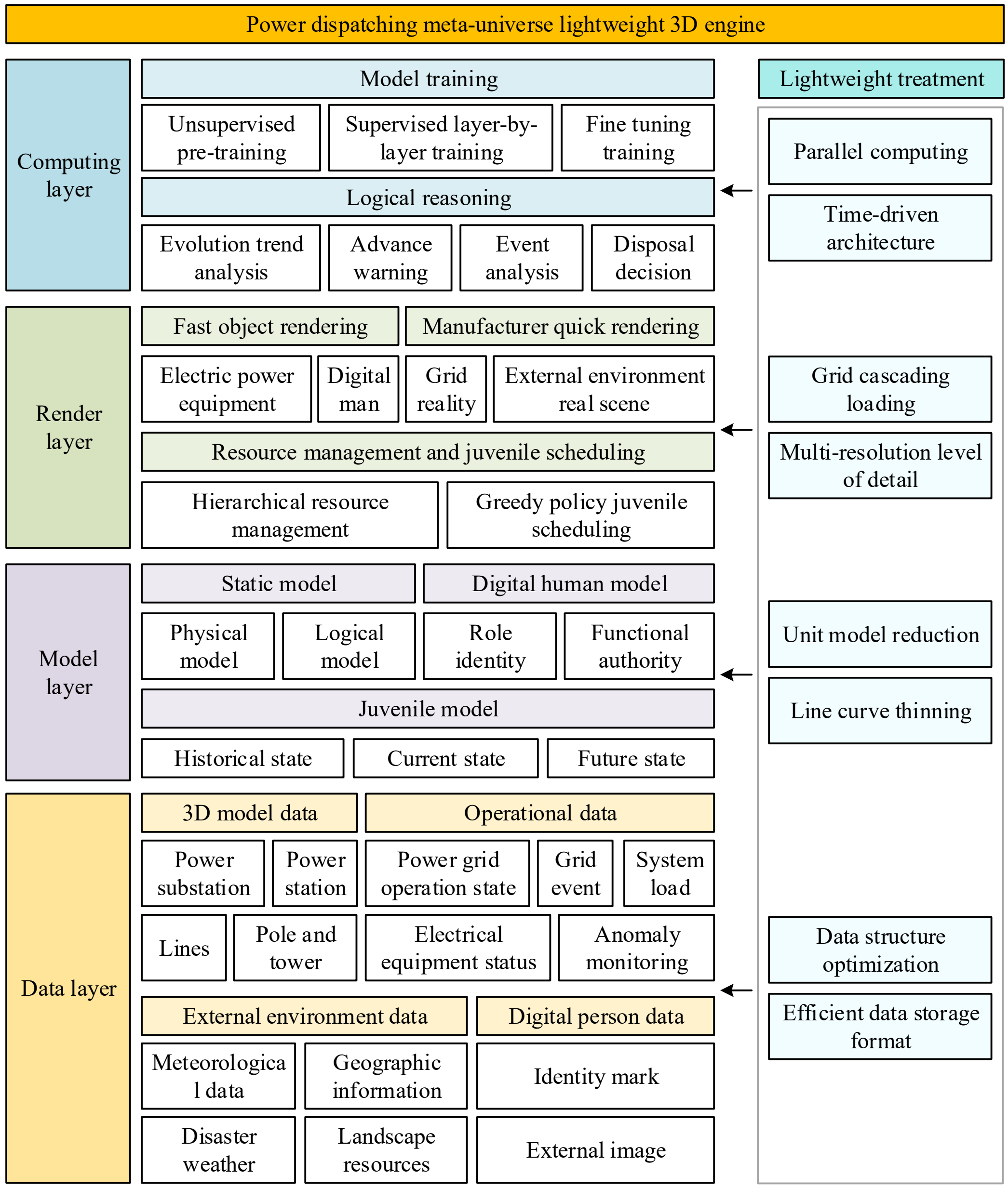

Fig. 1. Lightweight 3D Engine Design Architecture

2.3. One Grid Map Platform Architecture

2.3.1. Characteristics of the One Grid Map. One map of power grid refers to the comprehensive mapping of the physical power grid in digital space, and the construction of a digitized platform containing information on power grid equipment, operation status, meteorological environment, video monitoring and so on. It realizes the real-time convergence of grid equipment parameters, operation status and other information by integrating the data from the grid resource business center, enterprise-level measurement center and other digital platforms, and provides graphical service support for grid management, emergency command and business applications [15]. Its characteristics are as follows:

1) Comprehensiveness. One map of the grid covers detailed data of grid equipment of all levels of voltage from high-voltage to low-voltage, including substations, transmission lines, distribution lines and low-voltage stations, etc., realizing the digital management of all elements of the grid.

2) Real-time. Through real-time data aggregation, one map of power grid can dynamically display the operation status of power grid equipment, providing timely and accurate data support for power grid management.
3) Multi-dimensional. A map of the power grid not only contains static and dynamic information of the grid itself, but also superimposed on the meteorological environment, video surveillance and other multi-dimensional data, which provides richer information resources for power grid management.
4) Application. As a graphical service platform for cross-disciplinary integration and application, One Grid Map provides an intuitive and convenient operation interface for grid management and supports the lightweight construction of enterprise-level application scenarios.

2.3.2. One Grid Map platform design. The panoramic visualization of power grid enterprise production is of great importance in the digital construction of power transmission and distribution. Grid one map platform integrates multiple data systems to realize the comprehensive display and application of grid status, equipment status, process safety, emergency command, intelligent control of operators, intelligent equipment control and index control. This paper establishes a panoramic display platform for power grid production information supported by the grid lightweight 3D engine technology constructed in the previous paper. Relying on this platform can improve the effectiveness of decision-making suggestions and work efficiency, and also improve the decision-making, work efficiency and overall coordination of operation and maintenance, promoting the digital transformation of the energy industry and improving the overall operation level.

The One Grid Platform is a tool based on data collection, analysis and display, which can help commanders better understand the operation of the grid, formulate scientific and reasonable decision-making and scheduling plans, and improve the operation effect and economy of the grid. Through grid monitoring, commanders can understand the operating status and parameter data of the grid in real time, so as to deal with faults and optimize dispatching in time. Grid fault diagnosis locates and diagnoses faults and provides repair strategies by collecting and analyzing grid operation data. Grid load management enables load dispatch and energy supply strategy optimization by monitoring, analyzing and optimizing load data. Grid data analysis helps commanders understand the operating trend and changing law of the grid through visual display and in-depth analysis of historical data, providing a scientific basis for decision-making [16].

Through the collection of key data, transmission to the central processing center, real-time monitoring and analysis, the grid one map platform is able to detect potential energized problems and issue timely fault prompts. At the same time, the visualization interface intuitively displays the grid operation status and changes in the risk of energization, and the operation and maintenance personnel can remotely control the equipment and take preventive measures. Through these measures, it can improve the safety and reliability of the power grid, provide real-time data and operation interface for O&M personnel, and effectively reduce the risk of energization.

3. Two-tier optimal scheduling model with one map of the grid

As a unified whole composed of generation, transmission, transformation, distribution and use, the power grid requires mutual coordination and unified scheduling in terms of operational characteristics. With the increasing input of power generation and storage equipment, the continuous improvement of protection devices for security and stability of the transmission grid, the increasing access of demand response loads in the distribution grid, the expanding penetration of electric vehicles and their charging piles, and the expanding degree of coverage of data collection devices, the regional power grid is expanding in size and complexity, and the mode of operation is becoming more and more complicated. The scale of regional power grids is expanding, the operation mode is getting more and more complicated, and the connection and coupling between transmission and distribution networks are getting closer and closer. Relying on one map of power grid to realize multi-source coordinated optimal scheduling of power grid, it can better ensure the efficiency of power supply as well as the rationalization of energy utilization, and maximize the economic benefits of power grid scheduling.

3.1. Two-tier optimal scheduling model for power grids

In the grid multi-source cooperative optimal dispatch based on one map of the grid, for example, in a dispatch cycle a few days ago, the microgrid reports local renewable energy forecast power and load data to the distribution grid operator (DSO), and the DSO sends pricing information to the microgrid accordingly to guide it in arranging power scheduling to meet load demand. If the microgrid's local renewable energy output is insufficient, it will purchase power from other power-rich microgrids through the DSO, or dispatch local microturbine (MT) and energy storage system (ESS) resources. Conversely, it will trade its surplus power with other power-scarce microgrids through DSOs or dispatch local MT and ESS resources. In this case, each microgrid's own optimization strategy can be solved locally and only limited necessary information is exchanged through the DSO.

3.1.1. Upper layer DSO optimization model. The optimization objective of the upper layer model is to minimize the operating cost E^{DSO} of the DSO with the following objective function:

$$\min E^{DSO} = \sum_{t=1}^{24}\Big[c_t^{grid}P_t^{grid} - c_t^{grids}P_t^{grids} + \sum_{i=1}^{N}(c_{i,t}^{MGb}P_{i,t}^{MGb} - c_{i,t}^{MGs}P_{i,t}^{MGs}) + \sum_{j=1}^{M}c_t^{grid}P_{j,t}^{loss}\Big] \quad (12)$$

where P_t^{grid} and P_t^{grids} are the amount of electricity purchased and sold by the DSO to the transmission grid in time period t, c_t^{grid} and c_t^{grids} are the tariffs of electricity purchased and sold by the DSO to the transmission grid in time period t, and $P_{i,t}^{MGs}$ and $P_{i.t}^{MGb}$ are the amount of electricity purchased and sold by the DSO to MGi in time t, respectively. $c_{i,t}^{MGs}$ and $c_{i,t}^{MGb}$ are the tariffs of electricity sold and purchased by DSOs to MGi in time period t, respectively, N is the number of microgrids connected to the distribution network, $P_{j,t}^{loss}$ is the power loss of branch j in time period t, and M is the total number of branches [17].

The constraints of the upper level model are as follows:

$$P_{j,t} = V_j \sum_{jl} V_l (G_{jl}\cos\theta_{jl} + B_{jl}\sin\theta_{jl}) \quad j = 1, 2, \cdots, M \quad (13)$$

$$Q_{j,t} = V_j \sum_{l\in j} V_l (G_{jl}\sin\theta_{jl} - B_{jl}\cos\theta_{jl}) \quad j = 1, 2, \cdots, M \quad (14)$$

$$P_{j,t}^{loss} = | V_j V_l (G_{jl}\cos\theta_{jl} + B_{jl}\sin\theta_{jl}) - V_j^2 G_{jl} | \quad (15)$$

$$V_{\min} \le V_{j,t} \le V_{\max} \quad j = 1, 2, \cdots, M \quad (16)$$

$$P_{j\min}^{line} \le P_{j,t} \le P_{j\max}^{line} \quad j = 1, 2, \cdots, M \quad (17)$$

$$c_{i\min}^{MG} \le c_{i,t}^{MGb} \le c_{i,t}^{MGs} \le c_{i\max}^{MG} \quad i = 1, 2, \cdots, N \quad (18)$$

where $P_{j,t}$ and $Q_{j,t}$ are the active and reactive power at node j of the distribution network at time t, V_j and V_t are the first and last voltages of branch \$jl\$, G_{jl} and B_{jl} are the branch \$jl\$'s conductance and conductance parameters, and θ_{jl} is the phase angle difference between the first and last voltages of branch. $V_{\max}$ and $V_{\min}$ are the maximum and minimum values of voltage allowed in the system, respectively, $P_{j\max}^{line}$ and $P_{j\min}^{line}$ are the maximum and minimum transmitted power on line j, respectively, $c_{i\max}^{MG}$ and $c_{i\min}^{MG}$ are the maximum and minimum power trading prices between MGi and DSO set by DSO, respectively. Eqs. (13) and (14) are the distribution system tidal current equations, Eq. (15) is the branch power loss equation, and Eqs. (16) to (18) are the node voltage constraints, line power constraints, and tariff constraints of the distribution system, respectively.

3.1.2. Lower Level Microgrid Optimization Models. The energy in the microgrid not only has to satisfy its own load demand, but also needs to interact with the main grid, and if the interacting energy is too large it will cause fluctuation to the main grid. So the study of demand-side management and the utilization strategy of wind and light can allow the maximum dissipation of wind and light to minimize the net load and maximize the self-supply rate of the microgrid. Then:

$$\begin{cases} f_{DR} = \min \sum_{t=1}^{T} | P_L^{'}(t) - P_{vwb}(t) - P_{buy}(t) | \\ P_L^{'}(t) = P_L(t) + P_{DL}(t) - P_{CL}(t) \end{cases} \tag{19}$$

$$f_{zg} = \max\left(1 - \sum_{t=1}^{T} P_{buy}(t) / \sum_{t=1}^{T} (P_L^{'}(t) + P_{BES,c}(t)\right) \tag{20}$$

where P_{vwb} is the total power of wind and storage, f_{DR} is the minimum net load of the microgrid, f_{zg} is the self-supply rate, $P_L^{'}(t)$ is the load after the demand side management, $P_{CL}(t)$ and $P_{DL}(t)$ are the interruptions and shifted loads after demand-side management, $P_L(t)$ is the original load in time period t, and $P_{bay}(t)$ is the purchased power in time period t.

For the multi-objective results, this paper uses the fuzzy multi-attribute decision making method to select the best compromise solution o_{pt}, i.e.:

$$\begin{cases} A = \dfrac{F_j^{\max} - F_j^k}{F_j^{\max} - F_j^{\max}} \\ \gamma^k = \dfrac{\sum_{j=1}^{n} \gamma_j^k}{\sum_{k=1}^{m} \sum_{j=1}^{n} \gamma_j^k} \\ o_{pt} = \max(\gamma^k) \end{cases} \tag{21}$$

where γ_j^k is the satisfaction of the j objective function among the k feasible solutions, $F_j^{\max}, F_j^{\min}$ are the maximum and minimum of the j value of the objective function, respectively, F_j^k is the j value of the objective function among the k feasible solutions, and γ^k is the standard satisfaction of the kth feasible solution, and m and n are the number of feasible solutions and the number of objective functions, respectively.

Under the premise of considering demand-side management, relying on the forecast data of renewable energy from one map of the grid, this is used to realize microgrid dispatch optimization from the economic and environmental protection perspectives.

1) Comprehensive cost of microgrid. The operation and maintenance cost of each device, the interaction cost with the larger grid and the subsidy for demand response are required as the cost of microgrid operation, which is expressed as:

$$\begin{cases} F_1 = \min\left\{ \sum_{t=1}^{24} \begin{bmatrix} C_F(t) + \varepsilon(P_{DL}(t) + \\ P_{CL}(t)) + C_{grd}(t) \end{bmatrix} + C_{OM} \right\} \\ C_{OM} = C_{WT} + C_{BES} + C_{PV} + C_{MT} + C_{FC} \\ C_F(t) = \frac{C_{gas}}{L_{hv}} \left(\frac{P_{MT}(t)}{\eta_{MT}} + \frac{P_{Ec}(t)}{\eta_{Ec}} \right) \Delta t \end{cases} \tag{22}$$

where F_1 is the total cost of running the system for 24h, $C_{gid}(t) = aP_{buy}(t) - b\,|\,P_{sell}(t)\,|$, P_{sell} is the power sold to the larger grid, which is recorded as a negative value, and a,b are its price coefficients, respectively, C_{OM} is the sum of the maintenance costs of each micro-source, ε is the cost of the incentive response subsidy according to the power supply company, $C_F(t)$ is the fuel cost at the moment t, C_{gas} is the cost of the gas, and L_{hv} is the low calorific value of natural gas.

2) Environmental friendliness objective. In order to comply with the sustainable development concept of green electricity use, reducing pollutant emissions in the grid has become one of the main objectives nowadays. Renewable energy sources in microgrids also produce pollutants, but the pollutant emissions are greatly reduced compared to conventional power systems. The pollutants include CO_2, CO, NO_x and SO_2, which are mainly dominated by CO_2, CO, and so are expressed in terms of carbon emissions below. The objective function expression is:

$$F_2 = \min \sum_{t=1}^{24} \left\{ \sum_{\chi=1}^{n} \begin{pmatrix} W_{MT.\chi} P_{MT}(t) + \\ W_{g.\chi} P_{buy}(t) + W_{Fc.\chi} P_{Fc}(t) \end{pmatrix} \right\} \tag{23}$$

where F_2 is the total amount of pollutant emissions generated by the system operating for 24h, χ is the type of pollutant gas, and $W_{MT,x}, W_{g.x}$ and $W_{Fc,x}$ are the emission coefficients of the χ th type of pollutant gas corresponding to the micro-gas turbine, the power grid, and the fuel cell, respectively.

3) The power balance constraint can be expressed as:

$$P_{WT}(t) + P_{PV}(t) + P_{BES}(t) + P_{MT}(t) + P_{Fc}(t) = P_L^{'}(t) \tag{24}$$

4) The unit output constraint can be expressed as:

$$P_j^{\min} \le P_j(t) \le P_j^{\max} \tag{25}$$

where $P_j(t)$ is the unit output, $P_j^{\min}$ is the minimum value of the output of the j th unit, and $P_j^{\max}$ is the maximum value of the output of the j th unit.

5) The energy storage battery constraint can be expressed as:

$$\begin{cases} 0 \le P_{BES.c}(t) \le P_{BES.c}^{\max}(t) \\ 0 \le P_{BES.d}(t) \le P_{BES.d}^{\max}(t) \\ S_{OC}^{\min} \le S_{OC}(t) \le S_{OC}^{\max} \end{cases} \tag{26}$$

Where $P_{BES,c}^{\max}$ and $P_{BES,d}^{\max}$ are the maximum charging and discharging power of the battery, respectively.

6) If the microgrid interacts with the larger grid with too much power, the power system stability will be affected, so there should be some limitations. The transmission power constraint can be expressed as:

$$P_{out}^{\min}(t) \le P_{out}(t) \le P_{out}^{\max}(t) \tag{27}$$

Where $P_{out}^{\max}, P_{out}^{\min}$ are the upper and lower limits of the line transmission power allowed, and $P_{out}(t)$ is the grid transmission power at the t moment.

3.1.3. Joint scheduling with two-tier optimization. After completing the establishment of the optimization model at the upper DSO layer and the optimization model at the lower microgrid layer, the optimization results of these two layers are organically integrated in order to achieve the optimal scheduling of the whole grid system. In implementing the two-layer optimal scheduling strategy, a collaborative approach is used.

The upper-layer scheduling model acts as a leader and provides key boundary conditions to the lower-layer scheduling model, which provide clear guidance to the lower-layer model in developing the microgrid output plan and the exchanged power plan with the external grid. On this basis, the lower-layer microgrid optimization scheduling model plays its role of fine-tuned execution by developing detailed microgrid operation plans based on the boundary conditions provided by the upper layer. These plans not only include the power allocation of each microgrid, but also cover the power exchange strategy with the external grid. Once these plans are developed, they are fed back to the upper layer DSO optimized dispatch model. The upper layer model receives the data fed back from the lower layer and uses these data as new input conditions for updating and optimizing its internal model. Through this process, the upper layer model is able to further adjust and optimize its decisions based on more comprehensive information and more refined scheduling plans to better fit the operational needs of the entire system.

Through this repeated iteration and optimization between the upper and lower layers, it ensures that the whole system can achieve the optimal operation within the global scope, realizes the synergy between the two layers, and effectively realizes the optimal scheduling of distribution grids with multiple microgrids accessed under the one map of the power grid.

3.2. Co-optimized scheduling based on HPSOs

3.2.1. Hybrid particle swarm optimization algorithm:

1) Particle swarm optimization algorithm. Let the randomly initialized dust production m particles, each particle is a d -dimensional vector. The current position of the i th particle is x_i, the current velocity of the i th particle is v_i, the optimal position searched so far by the i th particle is p_{best}, the optimal position searched so far by the whole swarm of particles is g_{best}, the superscript denotes the iteration number of times, the velocity-position of the particle, and the update formula is as follows:

$$v_i^{t+1} = wv_i^t + c1r1(p_{best}^t - x_i^t) + c2r2(g_{best}^t - x_i^t) \tag{28}$$

$$x_i^{t+1} = x_i^t + v_i^{t+1} \tag{29}$$

Where $i = 1, 2, \cdots, m$, w is the inertia weight, taking the value range of 0.45~0.85, $c1, c2$ is called the learning factor or the acceleration factor, taking $c1 = c2 = 1.0$, and $r1, r2$ are the random numbers uniformly distributed between (0,1).

Among the parameter settings of the particle swarm, the inertia factor w is the most important, which directly affects the optimization performance of the algorithm. A larger w enhances the global search ability of the algorithm and facilitates jumping out of local minima, while a smaller w enhances the local search ability of the algorithm and facilitates its convergence. In order to obtain a more reasonable value of w this paper adopts a linearly decreasing strategy for the inertia factor, i.e., it is linearly decreasing to a smaller value by starting with a larger value, i.e.:

$$w = w_{\max} - Iter * (w_{\max} - w_{\min}) / maxIter \tag{30}$$

Where $w_{\max}$ is the maximum weighting coefficient, $w_{\min}$ is the minimum weighting coefficient, $Iter$ is the current iteration number, and $maxIter$ is the total iteration number. In addition, in order to prevent particles from flying out of the search space, it is necessary to limit the velocity range $[v_{\min}, v_{\max}]$ and the position range $[x_{\min}, x_{\max}]$ for particles to fly out of the search space, and when particles fly out of the boundaries, the particles are placed back to the boundaries and the particle velocities are changed so that the particles return back to the search space within the search space [18].

2) Immunization mechanism. The antibody pairs in the immunization mechanism are the particles of the PSO algorithm, which are two designations of the same concept. The degree of matching between antibodies and between antigens and antibodies can be described by affinity, while the inhibitory and promotional effects on antibodies are realized by relying on individual concentrations.

Let the immune system consist of M antibodies, each with n genes. Assuming that there are a total of S mutually unequal gene characteristic values on the j th gene, the information entropy $H_j(M)$ of the j th gene of the immune system is:

$$H_j(M) = \sum_{i=1}^{s} -p_{ij} \ln p_{ij} \tag{31}$$

where p_{ij} is the probability that the allele of the i th antibody appears on the j th gene. The population diversity of the immune system can be expressed as:

$$H(M) = \frac{1}{n} \sum_{j=1}^{n} H_j(M) \tag{32}$$

Define the affinity ay_w between antibody v and antibody w as follows:

$$ay_{vw} = \frac{1}{1 + H(2)} \tag{33}$$

Where $H(2)$ is currently mostly based on antibodies v and w, and its value is obtained using the above information entropy formula. Affinity is a measure of the degree of similarity between antibodies and between antibodies and antigens. The larger ay_{vw} is, the more affinity, or similarity, between the two antibodies v and w. $H(2)$ is used to represent the distance between antibodies, which can be calculated by information entropy or other methods. As long as the following two conditions are satisfied:

$H(2) \geq 0$ and $H(2) = 0$, the genes of the two antibodies are identical.

The greater the genetic difference between the two antibodies, the greater the value of $H(2)$.

For different encoding mechanisms, different methods can be used to calculate $H(2)$. In real number encoding, the method of calculating the Euclidean distance between two antibodies can be used. Let antibody $v = (v_1, v_2, \cdots, v_n)$ and antibody $w = (w_1, w_2, \cdots, w_n)$, then we have:

$$H(2) = \sqrt{\sum_{i=1}^{n} (v_i - w_i)^2} \tag{34}$$

The affinity ax_v between an antigen and an antibody v is used to indicate how well the antibody recognizes the antigen. It can be made such that $a\alpha_v = F_v$, where F_v is the value of the fitness function of antibody v.

The concentration of antibody v in the population c_v is defined as follows:

$$c_v = \frac{1}{M} \sum_{w=1}^{M} ac_w, ac_w = \begin{cases} 1, & ay_w \geq T_{acl} \\ 0, & otherwise \end{cases} \tag{35}$$

Where T_{ac1} is a pre-given threshold value, which can be taken as 0.3 to 0.5.

The immune mechanism discriminates by adjusting the fitness, whose high value is retained and replicated, and whose low value will be replaced. In other words, antibodies with high adaptation and low concentration are promoted, while antibodies with low adaptation and high concentration are suppressed. As a result, the diversity of the population can be strongly maintained, preventing the PSO algorithm from premature convergence and falling into local optimization, and improving the system performance of the PSO algorithm.

3) Linear adjustment of learning factor. To improve the convergence performance of the algorithm, the learning factor is linearly adjusted in this paper. In the early stage of calculation, the value of c_1 is large and the value of c_2 is small, and the particle swarm is based on the historical position of each particle, and the strong global search ability is used to quickly traverse the entire solution area to obtain the optimal position, and in the later stage of calculation, the value of c_1 is small, and the value of c_2 is large, and the particle swarm update is based on the global optimal particle position, which effectively improves the convergence accuracy and speed of the algorithm [19]. The linear adjustment strategy for learning factors can be expressed as:

$$c_1^* = c_{1\max} - (c_{1\max} - c_{1\min}) / t_{\max} \times t \tag{36}$$

$$c_2^* = c_{2\min} + (c_{2\max} - c_{2\min}) / t_{\max} \times t \tag{37}$$

4) Linear combination velocity and adaptive position update. When the algorithm is in the global search stage, the individual optimal and group optimal linear combination speed updating strategy can effectively improve the reliability of the PSO algorithm's exploration capability and solution. The particles will adjust the influence between particles from this linear combination to update the speed. The linear combination speed update formula is:

$$v_{ij}^{k+1} = \begin{cases} \omega v_{ij}^k + c_1 r_1 \left(\dfrac{\rho best_{ij}^k + \gamma best_j^k}{2} - x_{ij}^k \right) + c_2 r_2 \left(\dfrac{\rho best_{ij}^k - \gamma best_j^k}{2} - x_{ij}^k \right) & f(gbest^k) \le \alpha \\ \omega v_{ij}^k + c_1 r_1 (\rho best_i^k - x_i^k) + c_2 r_2 (gbest_j^k - x_{ij}^k) & f(gbest^k) > \alpha \end{cases} \tag{38}$$

When performing global search, $pbest_{ij}^k$ and $gbest_j^k$ in the PSO algorithm are replaced by $(pbest_{ij}^k + gbest_j^k)/2$ and $(pbest_{ij}^k + gbest_j^k)/2$ to update the particle velocity, respectively. Used when performing a localized search. The linear combination expands the flight region of the particles and increases the likelihood that the algorithm will find a high-quality solution during the global search.

The adaptive position update strategy has different exploration and exploitation capabilities. Using different position update formulas in the exploration and exploitation phases can improve the overall performance of the algorithm. The position update formula can ensure the local exploration capability of the algorithm and help the algorithm to jump out of the local optimum, while the introduction of inertia weights into the position update formula can improve the accuracy of the solution, which can help to speed up the convergence speed of the algorithm and improve the global exploitation capability of the algorithm. The adaptive position update formula is:

$$x_{ij}^{k+1} = \begin{cases} w x_{ij}^k + (1-w) v_{ij}^{k+1} & f(gbest^k) \le \alpha \\ x_{ij}^k + v_{ij}^{k+1} & f(gbest^k) > \alpha \end{cases} \tag{39}$$

The above equation expresses the extent to which the current particle's optimization speed affects the subsequent particle's speed, thus acting on the particle's optimization ability. The $w x_{ij}^k + (1-w) v_{ij}^{k+1}$ adds the effect of inertia weights to improve the algorithm's global search performance, and $x_{ij}^k + v_{ij}^{k+1}$ maintains the algorithm's performance in local search.

3.2.2. Collaborative optimization of the scheduling process. Based on the above improvement strategies of PSO algorithm, this paper proposes a hybrid particle swarm algorithm (HPSO) for solving the multi-source collaborative two-layer optimal scheduling model of a single map of the grid. The

HPSO algorithm adopts an immune mechanism to differentiate between particles in order to maintain the particle swarms always distributed in the solving plane more evenly, avoiding the particles from falling into the local optimum. A linear adjustment learning factor is introduced to accelerate the convergence speed of the particles, and a linear combination of speed and adaptive position updating strategy is used to balance the self-cognitive and social cognitive abilities of the particles, so as to update the speed and position of the particles. Figure 2 shows the flow of the HPSO algorithm to solve the two-layer optimal scheduling model.

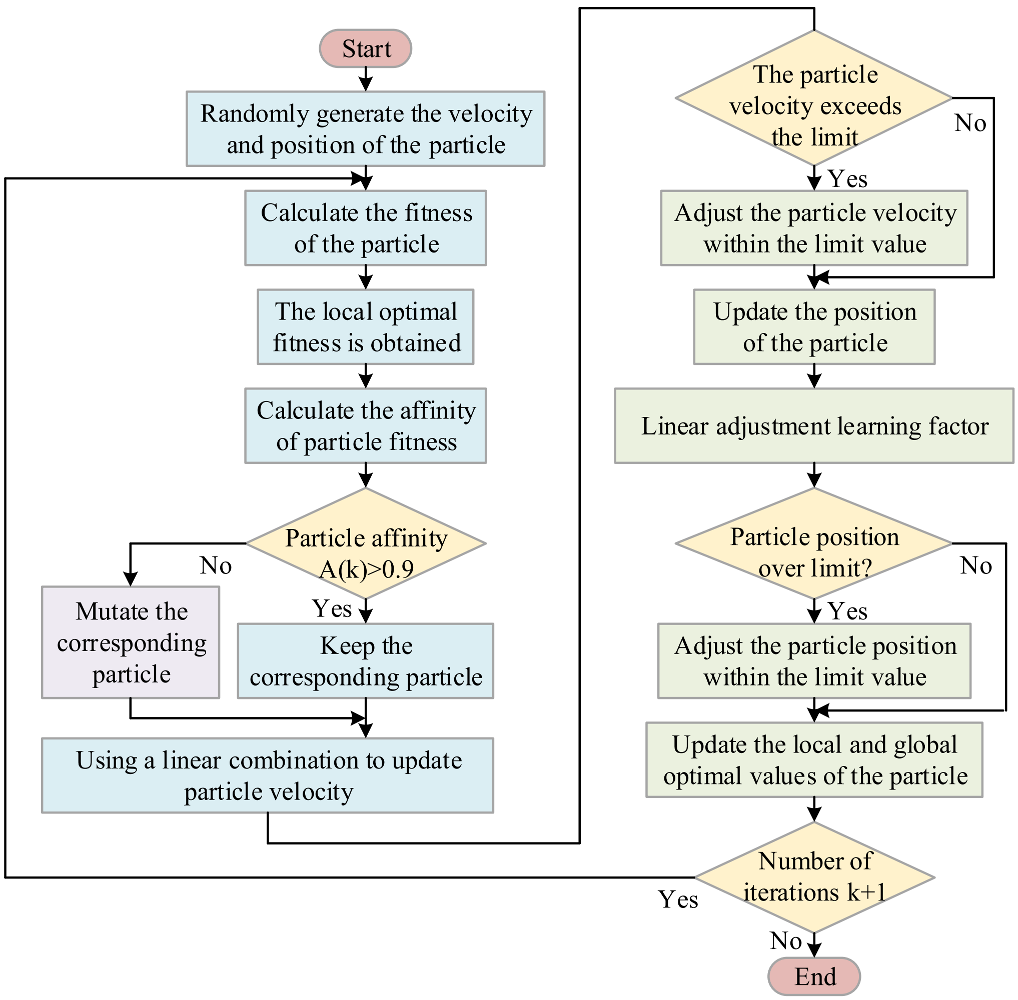

Fig. 2. The process of solving the double layer optimization scheduling model

In this paper, the process of using HPSO algorithm to determine the two-tier optimal scheduling model for one map of the power grid is as follows:

Step1 Initialization of the algorithm. In this step, the economic parameters of controllable micro-sources and load demand, power constraints, number and dimensions of particles and maximum number of iterations of the algorithm as well as parameters need to be entered.

Step2 Initialize the population. The particles and dimensions in the algorithm are randomly initialized according to the constraints of different microsources, and all the particles must satisfy the actual power constraints of the microsources, while the first N-1 dimensions of the algorithm randomly generates the positions and velocities of the particles, and the Nth dimension is the difference between the sum of the power generation of all the microsources and the load demand as calculated by Eq. The states of different microsources represented by the particles after k iterations at different moments can be expressed as:

$$X^{(k)}=\begin{bmatrix} x_i^{(k)}(1,1) & x_i^{(k)}(2,1) & \cdots & x_i^{(k)}(N,1) \\ x_i^{(k)}(1,2) & x_i^{(k)}(2,2) & \cdots & x_i^{(k)}(N,2) \\ \vdots & \vdots & & \vdots \\ x_i^{(k)}(1,T) & x_i^{(k)}(2,T) & \cdots & x_i^{(k)}(N,T) \end{bmatrix} \tag{40}$$

Step3 Calculate the solutions of the objective function corresponding to different unit powers after k iterations according to the formula given before.

Step4 Find the smallest solution of the objective function p_{best}, calculate the geometric distance between the other solutions and p_{best} and judge the size of the distance, and perform the mutation operation if the distance is small.

Step5 Use linear combination to update the particle's velocity v_i.

Step6 Judge whether the velocity of the particle exceeds the boundary, if it does, limit it to the maximum velocity.

Step7 Update the position of the particle x_i, which is the power of the ith microsource, according to the adaptive strategy.

Step8 Judge whether the position of the particle is out of bounds, if it is out of bounds, limit it to the maximum power of the microsource.

Step9 Judge whether the sum of all micro-sources power is equal to the load demand within the constraints, according to the power constraints of different micro-sources to limit the position of the particle, if it is less than the load demand, the value outside the range under the islanding mode of operation will be made up by the energy storage battery. If the storage battery has reached the power limit, the load is randomly allocated by other micro-sources without reaching the climbing power limit. The value outside the range under the grid-connected operation mode is made up by the main grid, and the objective function under the current power allocation is recalculated.

Step10 $k=k+1$, if $k<k_{\max}$, return to Step5.

Step11 From all the current objective function solutions p_{best}, derive the solution of the global lowest objective function g_{best}, which is the optimal value of the grid two-tier optimal scheduling.

4. Simulation of two-tier optimal scheduling with one map of the power grid

The large-scale access of renewable energy generation, the rapid development of distributed energy, energy storage, electric vehicles and other interactive energy facilities, and the gradual maturation and rapid development of the power market have led to great changes in the operation and management mode of the power grid. The construction of a grid platform with smart grid as the core, renewable energy as the foundation, Internet technology as the link, and a high degree of integration of energy and information to realize the coordinated and interactive optimized operation of "source-grid-load-storage" has become a strategic choice for the further development of many electric power enterprises.

4.1. Validation of the effectiveness of the HPSO algorithm

4.1.1. Test function analysis. In order to verify the performance of the HPSO algorithm, five benchmark functions, Sphere, Rosenbrock, Griewank, Rastrigin and Ackley, are selected to test the performance of the algorithm. Sphere and Rosenbrock are single-peak functions with a unique local extreme point (global optimum point), which can be used to test the algorithm's ability to find the optimal point and convergence speed, and Griewank, Rastrigin, and Ackley are multiple-peak functions with multiple local extreme points and a unique global optimum point, which can be used to test the algorithm's ability to jump out of the local optimum point.

The standard PSO algorithm, linearly decreasing inertia weighted particle swarm (LPSO) algorithm are selected for comparison experiments to test the performance of the HPSO algorithm in this paper. The initial population size of all algorithms is set to 50, the inertia weights take the value range of

[0.45,0.85], both learning factors are set to 1.5, and the number of iterations is 1000. The above three algorithms were run independently for 30 times, and the results of the algorithms solving the test function are shown in Table 1.

From the comparison results of the data in the table, it can be seen that compared with the PSO and LPSO algorithms, the HPSO algorithm shows better solving ability in solving the test function. The optimal value, the worst value and the average value of the HPSO algorithm in solving the single-peak function and the multiple-peak function are better than those of the PSO and the LPSO algorithms, which means that the algorithm of the present paper has a better accuracy of finding the optimal value. For the three benchmark test functions of Sphere, Rosenbrock, and Rastrigin, the HPSO algorithm is able to find its theoretical optimal solution 0.

Table 1. The algorithm solves the results of the test function

Functions	Algorithm	Best	Worse	Means
Sphere	PSO	8.54E-11	2.64E-03	7.41E-05
	LPSO	5.72E-38	6.89E-13	5.31E-19
	HPSO	0.000	1.34E-38	7.78E-56
Rosenbrock	PSO	3.45E+02	3.15E+05	3.68E+03
	LPSO	2.16E+01	1.24E+02	5.29E+01
	HPSO	0.000	9.64E+01	2.48E+01
Griewank	PSO	9.42E-03	7.75E+01	2.52E-02
	LPSO	3.06E-09	3.74E-01	5.43E-03
	HPSO	1.514	8.62E-03	1.26E-07
Rastrigin	PSO	2.36E+01	7.57E+01	5.39E+01
	LPSO	1.68E+01	1.03E+02	7.23E+01
	HPSO	0.000	4.31E+01	3.16E+01
Ackley	PSO	9.15E-01	1.764	1.153
	LPSO	4.53E-15	2.016	2.29E-07
	HPSO	2.48E-20	5.47E-13	6.16E-16

4.1.2. Algorithm effectiveness analysis. In order to further verify the scientificity and effectiveness of the HPSO algorithm proposed in this paper in solving the multi-source cooperative two-layer optimal scheduling problem in a single map of the power grid, the comparison results of the iteration results and the number of iteration times obtained after the optimization and solution of the planning model using the Genetic Algorithm (GA), the Hybrid Frog Leaping Algorithm (SFLA), the PSO algorithm and the HPSO algorithm of this paper, respectively, are shown in Fig. 3.

Comparison results show that when using SFLA algorithm to solve the grid two-layer optimal scheduling planning model established in this paper, the algorithm falls into local optimum after about 10 iterations, and the total planning cost obtained is 8.82*106 yuan. The number of iterations to solve the model using the genetic algorithm is 84, and the optimal result is 8.41*106 yuan, and the number of iterations, convergence speed, and search accuracy of the algorithm's solution are inferior to that of the PSO algorithm. In addition, comparing the PSO algorithm with the HPSO algorithm in this paper, the total planning cost obtained by using the PSO algorithm is 7.96*106 yuan, and the number of iterations is 48 times. And the total planning cost obtained by using the HPSO algorithm proposed in this paper is 7.69*106 yuan and the number of iterations is 12 times. It can be seen that the HPSO algorithm in this paper greatly improves the convergence speed of the optimization algorithm and obtains results that are more in line with the economic benefits of optimal grid scheduling planning.

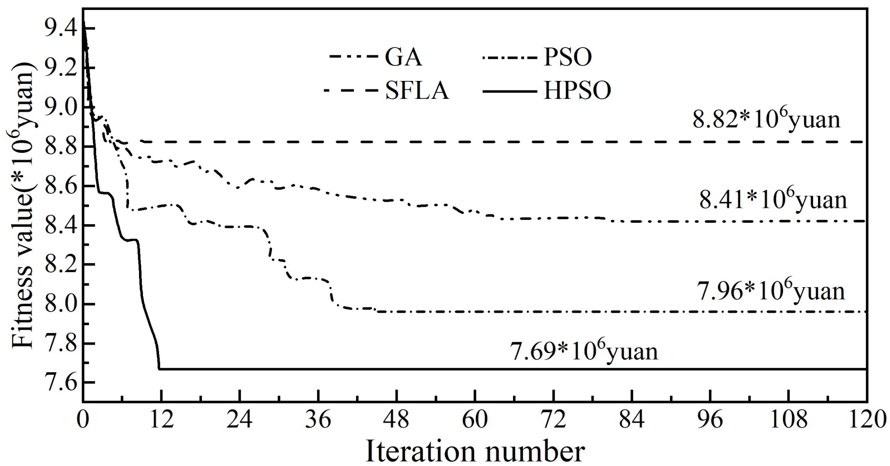

Fig. 3. The contrast between the results and the number of iterations

4.2. Simulation of two-tier optimal scheduling of power grids

4.2.1. Results of model runs. This paper is based on the one map platform of the grid, and its purpose is to better realize the optimal scheduling of the grid, which ensures the optimal scheduling economic efficiency, and the microgrid and environmental protection costs can also be optimized. Based on the consideration of uncontrollable residential electricity consumption, a two-layer optimal dispatch model of the grid is established from the supply side and the demand side. In this paper, the HPSO algorithm is utilized to obtain the optimal scheduling results, and in order to verify the effectiveness of the algorithm, three different scenarios (Scenarios A, B, and C) are set up in this paper, i.e., the GA, SFLA, and HPSO algorithms are utilized to solve the grid bi-layer optimal dispatch model, and a fourth scenario (Scenario D) is additionally set up, which is the optimal scheduling of the grid bi-layer under the consideration of uncontrolled residential power consumption. The initial scale and correlation coefficients of each algorithm are set optimally, and different algorithms are run independently to obtain the optimal scheduling results of the model. Figure 4 shows the load curves before and after considering uncontrollable residential electricity consumption, the grid operation costs under different scenarios are shown in Figure 5, and the evaluation of grid operation results is shown in Table 2.

Comparing Scenario A, Scenario B and Scenario C, the results of the grid two-layer optimization model obtained by solving the HPSO algorithm in this paper are better than those of the GA and SFLA algorithms, and the operating costs are reduced by 8.29*106 and 4.36*106 yuan, respectively, which illustrates the superiority of the HPSO algorithm proposed in this paper. Under different tariff mechanisms, the equivalent load after user participation in demand response as well as the original load curve changes are more obvious, it is obvious that the time-sharing tariff formulated on the basis of user-side load has a better effect of peak shaving and valley filling, and the difference between peaks and valleys is adjusted from 499.1kW to 377.8kW. Based on the consideration of uncontrollable residential electricity consumption, it can better realize the efficient scheduling of the grid and realize the effective use of energy.

With the same algorithm, demand side management is considered. Scenario C reduces the economic and environmental costs by 51.78% and 23.07%, respectively, compared to Scenario D. The total cost is reduced by 8.66*106 yuan. In Scenario C, which considers uncontrollable residential electricity consumption, the penetration of renewable energy increases significantly. The reason for this is that the renewable energy sources prioritize the transmission of power to the uncontrollable end of the population in order to meet the load demand of the population and then store the excess power after meeting their own load demand. This also leads to a certain extent to a significant increase in the output of micro gas turbines, so the economic cost of some microgrids appears to increase, but due to the total cost optimization of microgrids is more obvious, which leads to a significant reduction in the total cost of microgrids. From the above, it can be seen that the consideration of uncontrollable residential electricity loads in the microgrid group can significantly improve the economy and environmental protection, relying on a single map of the grid to better balance the energy scheduling of microgrids, and also promote the energy enterprises to achieve the optimal economic efficiency.

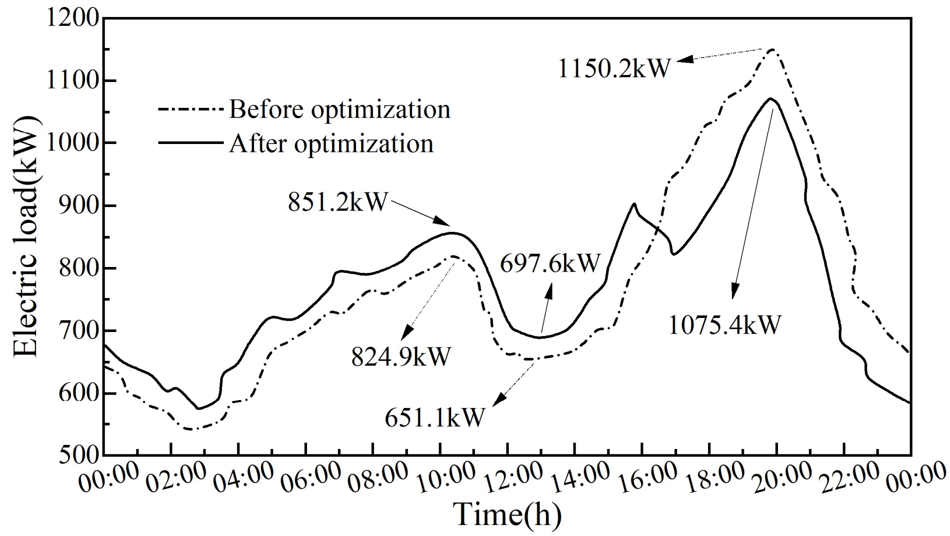

Fig. 4. Consider uncontrollable residents' electricity

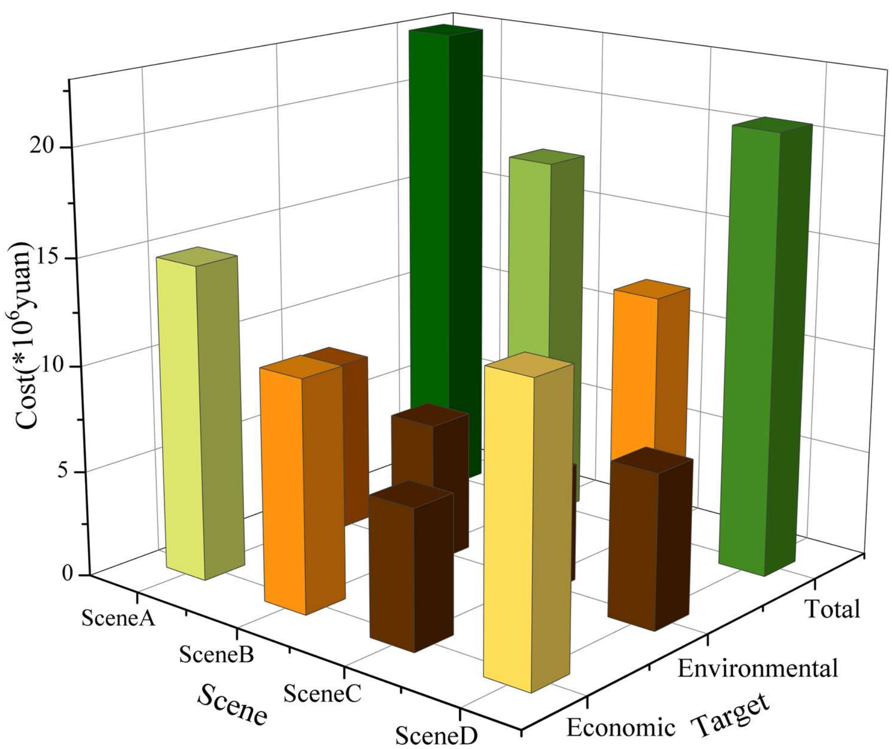

Fig. 5. Operating costs of power grid in different scenarios

Table 2. Assessment of running results

Scene	Economic cost (yuan)	Environmental cost (yuan)	Total cost (yuan)	Permeability	User satisfaction
A	1.48*107	8.16*106	22.96*106	0.807	0.872
B	1.09*107	6.63*106	17.53*106	0.814	0.872
C	6.51*106	5.57*106	12.08*106	0.826	0.878
D	1.35*107	7.24*106	20.74*106	0.768	0.912

4.2.2. Demand response results. In the lower microgrid optimization model, the correlation between the supply side and the demand side is fully considered, and the changes in the purchased and sold power, transferable load and curtailable load before and after the demand response are solved, and the results of the demand response are shown in Fig. 6. Fig. 6(a)~(c) shows the curves of the changes of purchased and sold power, transferable load and curtailable load before and after the demand response, respectively.

Based on the demand response results, the following conclusions are drawn:

From Fig. 6(a), it can be seen that after demand response, the system reduces the purchased power demand during the peak load period and increases the sold power during the low load period, which realizes the balance between supply and demand of the system.

From Fig. 6(b), it can be seen that the fluctuation of transferable load is significantly reduced and the load curve becomes smoother. Through demand response, part of the load in the peak period is transferred to the low valley period, thus reducing the load pressure in the peak period and improving the smoothness of system operation.

From Fig. 6(c), it can be seen that the curtailable load is reduced in most of the time, especially in the peak load period, thus reducing the system pressure.

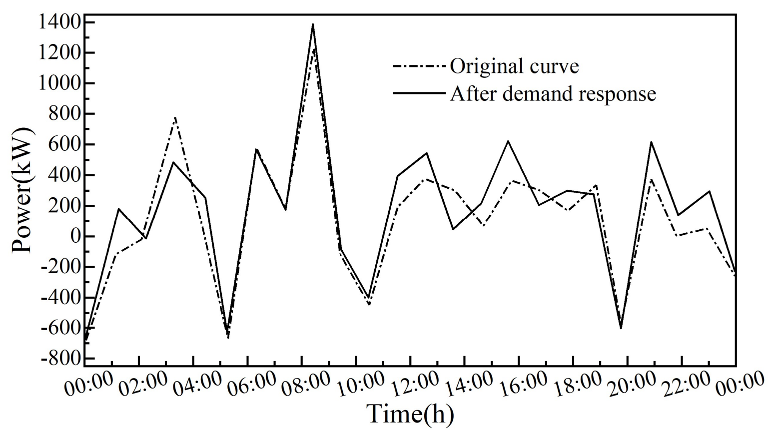

(a) Purchase and sale power

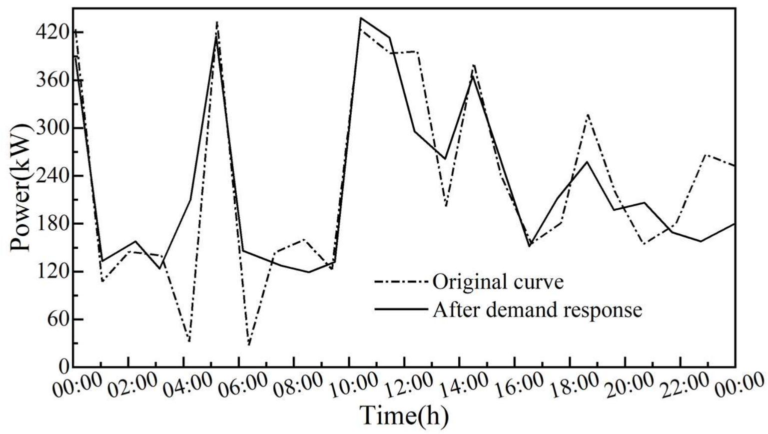

(b) Transferable load

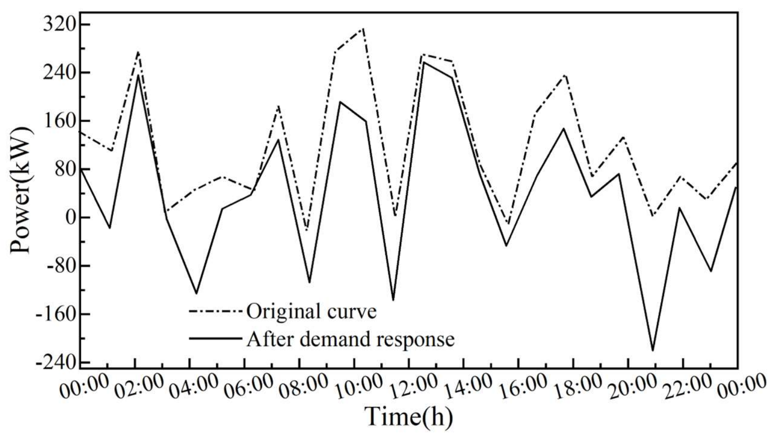

(c) Reducible load

Fig. 6. Demand response for the power grid

From the above results, it can be seen that the purchased and sold power, transferable loads and curtailable loads of the microgrid are significantly optimized through demand response. Table 3 shows the comparison of optimization results of GA, SFLA and HPSO. As can be seen from the table, compared with the optimization results of GA and SFLA algorithms, the HPSO algorithm solves to obtain a reduction of about 17.11% and 10.64% in the investment cost, respectively, and a reduction of 0.52*104 and 0.46*104 yuan in the maintenance cost, respectively, and the comfort level of power consumption and energy comfort have been significantly improved, and the comprehensive comfort level has been increased by 17.84% and 15.84%, respectively. Comparison results show that the optimization results obtained by using the HPSO algorithm solution can make the economic benefits in terms of maintenance higher while keeping the equipment running efficiently. And it can better balance the economic benefits and user experience on the whole, and improve the comprehensive operation effect of microgrid.

Table 3. Optimization results of different algorithms

Parameter	GA	SFLA	HPSO
Investment cost (yuan)	1.52*107	1.41*107	1.26*107
Maintenance cost (yuan)	9.64*104	9.58*104	9.12*104
Using electric comfort	0.873	0.891	0.952
Using energy comfort	0.516	0.523	0.685
Comprehensive comfort	0.695	0.707	0.819

4.2.3. Typical Time Period Analysis. In order to study the ultra-short-term peaking and insufficient climbing problems of the grid system under the platform of one map of the grid, a study is carried out on the morning peak hours of 6:30~8:30, when the renewable energy sources change drastically, and the time interval is set to 5 min. two cases are set up in this paper to discuss the practical application of the multi-source coordinated two-layer optimal scheduling. Scenario A only considers power system power balance and reserved reserve margin, while Scenario B comprehensively considers multi-source flexible resource coordination optimization. The peak-up and peak-down capacities and residual capacities at typical time periods under different scenarios are shown in Figs. 7 and 8.

As can be seen from Figure 7, under time periods 06:40~06:50, 07:05~07:30, and 08:10~08:25, Scenario A has insufficient up-peaking capacity, which is prone to the risk of load cutting and increases the cost of penalizing insufficient peaking capacity. Scenario A has significantly higher peaking capacity for time periods 06:30~06:35 and 07:45~08:10, which smoothes the intraday peak-to-valley difference and ensures the safe and stable operation of the power system.

As can be seen from Fig. 8, the remaining capacity of up- and down-peaking for Scenario A is roughly ±630 MW, and the remaining capacity of down-peaking for 07:35 is about 0 MW, which is a serious shortage of system down-peaking capacity, and the remaining capacity of up-peaking for 08:10 is about 0 MW, which is a serious shortage of system up-peaking capacity. In Scenario B, for the time periods 06:30~07:35 and 07:55~08:25, the incremental downhill remaining capacity is about 1,400 MW, and for the time period 07:35~08:00, the incremental uphill remaining capacity is about 1,150 M W. The overall remaining capacity of the system has been greatly increased, which meets the requirements for safe and stable operation of the power system in the ultra-short-term time period.

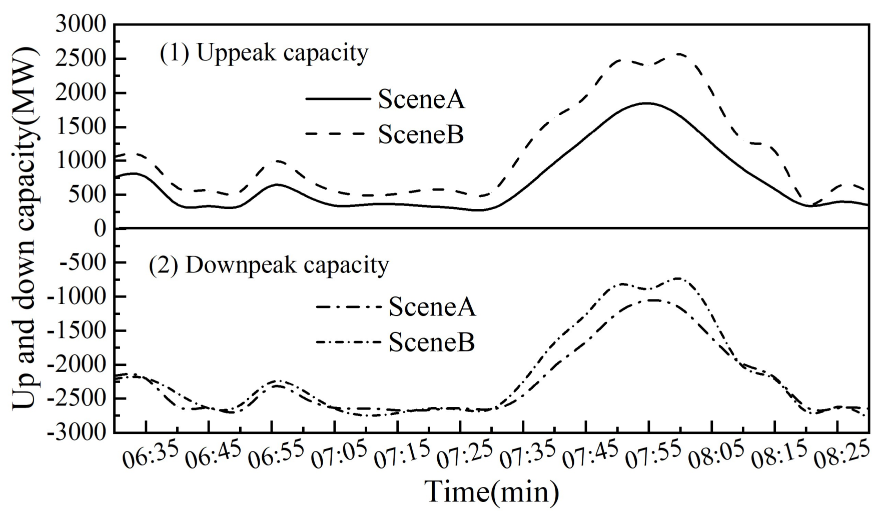

Fig. 7. Typical time up and down capacity

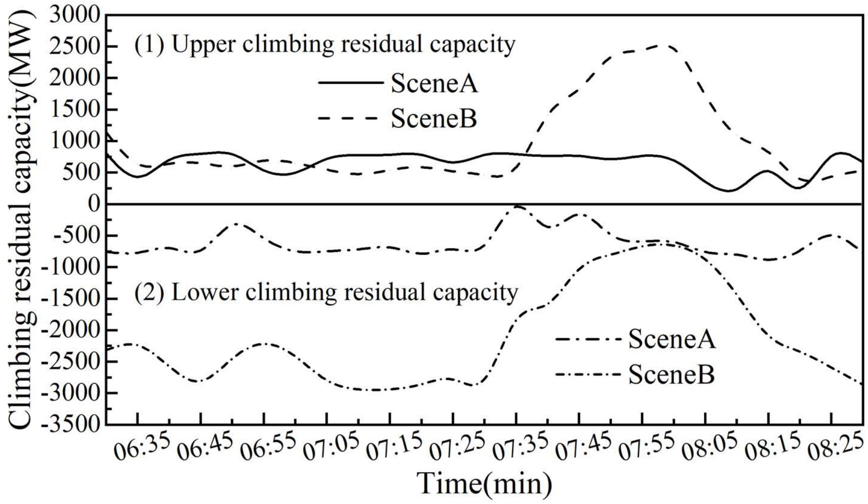

Fig. 8. The typical period of the climb of the residual capacity

4.3. Testing of the One Grid Map platform

4.3.1. Development environment setup. Based on the lightweight grid three-dimensional engine technology, the establishment of the grid a map production information panoramic display platform system, the construction of the development environment includes the following:
1) Java runtime environment installation.
2) Tomcat application server environment installation, version omcat8, for running GeoServer spatial data services and 3D grid system services.
3) PostgreSQL database installation, version number PostgreSQL 9.4.12, used to store relevant data from the electric power big data platform, and at the same time provide data source to the power grid one map production information panoramic display platform system.
4) GeoServer Map Service Installation, version number is GeoServer v2.1, which is used for deploying the relevant map data of the project study area and publishing the map service so as to be integrated into the One Grid Map Production Information Panoramic Display Platform System.
5) OpenLayers, Cesium map client package setup, used for calling GeoServer related map services and 2D/3D rendering by the client of Grid One Map system.
6) Installation of Eclipse development environment, which is used for the functional design, development and testing of one map production information panoramic display platform system for power grid.

4.3.2. Platform performance testing. System performance testing is performed by using the LoadRunner tool. The first step is to run LoadRunner by double clicking on the folder where it is stored, /bin/loadrunner.bat. The second step is to click on the file and select Open to open the stored test script. Step 3 Click Thread Groups and set the number of threads (concurrency) and runtime in the interface. Step 4, click Result Tree and Aggregate Reports to view the performance report. Table 4 shows the results of the server resource utilization test.

In the performance test of Grid One Map production information panoramic display platform system, its operation response speed is fast and the system runs stably. In this performance test, a total of 7 single script test cases were executed with 100 virtual users concurrently. The average response time of the scenarios of the 3D digital scene module, spatial 3D calculation module, spatial 3D analysis module, other modules, grid engineering module, basic function module and layer tree organization and management module is less than 3.5 seconds, which meets the requirements of the relevant indicators in the demand. In terms of system resource usage, the server resource usage is within the normal range. In this performance test, all test cases meet the requirements in the requirements and satisfy the system performance test requirements.

Table 4. Server resource utilization

Module	Server	CPU usage	Load	Response time
3D digital scene module	Application server	56.24%	3.57	3014.52ms
	Database server	16.38%	1.68	
Space 3Dl measurement module	Application server	44.72%	3.65	2417.38ms
	Database server	13.94%	1.24	
Spatial three-dimensional analysis module	Application server	60.16%	3.66	3142.79ms
	Database server	20.35%	1.74	
Other modules	Application server	50.17%	3.68	2306.26ms
	Database server	9.66%	1.25	
Power grid engineering can be modular	Application server	58.27%	3.73	2654.12ms
	Database server	19.35%	1.73	
Basic function module	Application server	55.49%	3.56	887.49ms
	Database server	18.21%	1.74	
Layer tree control module	Application server	50.42%	3.54	546.63ms
	Database server	16.38%	1.65	

5. Conclusions and outlook

5.1. Conclusion

Characterized by its massive heterogeneous data, huge computing power, high standard visualization needs and strong interactivity, power dispatching requires efficient data processing capability, advanced model rendering technology and rich interface support to adapt to diverse data types and complex business scenarios. In this paper, based on the lightweight 3D engine technology of power grid, we designed a panoramic display platform of production information on one map of power grid, and designed a two-layer optimal scheduling model on the platform, and introduced HPSO algorithm to solve the optimal scheduling of power grid. Relying on the grid one map can realize the double-layer optimal scheduling of the grid, better meet the demand of economic scheduling of the grid, and ensure the economic benefits of the grid enterprise, but also make the grid energy more rationalized.

5.2. Outlook

In the future, the system experience can be continuously improved by adding optional or adaptive functions of 3D model resolution under different network conditions and different hardware configuration conditions; increasing the physical rules of the real world in the engine, optimizing the form of multi-dimensional information display, and strengthening the sense of presence so that the dispatchers feel immersive. Integration of multi-system resources, such as synchronizing the virtual twin grid elements in the meta-universe with real images captured by surveillance or real-time monitoring data as a comparison.

Looking ahead, continue to explore in the research direction of deep integration of meta-universe and power dispatching. Explore more effective correlation expression methods for massive power dispatch data to cope with the complexity and correlation of the data. Explore multi-modal interaction technologies in the metaverse, such as gesture, speech recognition, brain-computer interface, etc., to realize efficient human-machine interaction. Explore the practice of clinical operation in virtual environment with virtual control of reality, and compose the information-physical fusion system of human-in-the-loop.

With the iterative development of artificial intelligence technology, in the future, it is possible to project the future short-term, medium- and long-term grid operation in the meta-universe based on the historical data of the grid or customized variable values, speculate on the impact of meteorological conditions, policy changes, changes in energy prices, changes in perceptions, and other environmental and social activities on the power grid, and respond in advance to scheduling strategies and disasters, failures, and so on. It is also possible to formulate investment and planning for the power system in the coming years and decades under the constraints of given objectives.

Acknowledgements

This work was supported by Science and Technology Project of SGCC (Research on the Verification of Power Dispatch Metaverse Architecture and Key Basic Technologies (5108-202312052A-1-1-ZN)).

References

[1] Rivera, J., Leimhofer, J., & Jacobsen, H. A. (2017). OpenGridMap: towards automatic power grid simulation model generation from crowdsourced data. Computer Science-Research and Development, 32, 13-23.

[2] Ashkezari, A. D., Hosseinzadeh, N., Chebli, A., & Albadi, M. (2018). Development of an enterprise Geographic Information System (GIS) integrated with smart grid. Sustainable Energy, Grids and Networks, 14, 25-34.

[3] Wu, K., Sun, D., Li, X., Jiang, Z., Niu, X., & Yang, J. (2017, April). Study of GIS-oriented graphical management system for power grid planning based on cloud service. In 2017 IEEE 2nd International Conference on Cloud Computing and Big Data Analysis (ICCCBDA) (pp. 504-508). IEEE.

[4] Bai, H., & Wang, Y. (2022). Digital power grid based on digital twin: Definition, structure and key technologies. Energy Reports, 8, 390-397.

[5] Sanchez-Hidalgo, M. A., & Cano, M. D. (2018). A survey on visual data representation for smart grids control and monitoring. Sustainable Energy, Grids and Networks, 16, 351-369.

[6] Rossi, B., & Chren, S. (2019). Smart grids data analysis: a systematic mapping study. IEEE Transactions on Industrial Informatics, 16(6), 3619-3639.

[7] Dhanalakshmi, J., & Ayyanathan, N. (2022, November). Geospatial Data Visualization of an Energy Landscape and Geographical Mapping of a Power Transmission Line Distribution Network. In International Conference on Computational Intelligence in Machine Learning (pp. 305-313). Singapore: Springer Nature Singapore.

[8] Zhang, L. (2021, November). Research and application of 3D GIS in the visualization and information management of power grid construction projects. In Journal of Physics: Conference Series (Vol. 2083, No. 3, p. 032024). IOP Publishing.

[9] Wang, H., Huang, Z., Zhang, X., Huang, X., wei Zhang, X., & Liu, B. (2022). Intelligent power grid monitoring and management strategy using 3D model visual computation with deep learning. Energy Reports, 8, 3636-3648.

[10] Xinghu, W., Hantuo, D., Yanfeng, W., Wenwei, Z., & Jingen, G. (2025). A Study of Automated Calibration Problems of Lightweight 3D Digital Models for Power Grid Engineering. International Journal of High Speed Electronics and Systems, 2540312.

[11] Medjroubi, W., Müller, U. P., Scharf, M., Matke, C., & Kleinhans, D. (2017). Open data in power grid modelling: new approaches towards transparent grid models. Energy Reports, 3, 14-21.

[12] Khalid, M. (2024). Energy 4.0: AI-enabled digital transformation for sustainable power networks.

Computers & Industrial Engineering, 193, 110253.

[13] Qingrui, L., Bixing, L., Shuze, G., Jiangping, Y., & Chaowang, W. (2023, October). Research on Fast Analysis Model of Power Big Data Integrating 3D Data Visualization Scene. In 2023 IEEE 3rd International Conference on Data Science and Computer Application (ICDSCA) (pp. 1400-1405). IEEE.

[14] Li, Y., Luo, J., Dong, C., & Feng, Y. (2022, December). 2D/3D Visualization Realization of Power Grid Operation Monitoring System Based on Big Data. In International Conference on Big Data Analytics for Cyber-Physical System in Smart City (pp. 337-345). Singapore: Springer Nature Singapore.

[15] Liloja Basheer & Ranjana P. (2025). A deep learning framework for intrusion detection system in smart grids using graph convolutional network. Engineering Research Express,7(1),015257-015257.

[16] Najet Hamdi. (2025). A hybrid learning technique for intrusion detection system for smart grid. Sustainable Computing: Informatics and Systems,46,101102-101102.

[17] Genfu Xiao,Huan Liu & Javad Nabatalizadeh. (2025). Optimal scheduling and energy management of a multi-energy microgrid with electric vehicles incorporating decision making approach and demand response. Scientific Reports,15(1),5075-5075.

[18] Yu Pan,Jin Wen,Ying Zhang,Shuangchao Qu,Chenglong Wang,Lan Yin... & Dingkang Zhang. (2025). Ultra-compact asymmetric polarization beam splitter based on hybrid plasmonic waveguide and subwavelength grating utilizing particle swarm optimization algorithm. Optics Communications,582,131624-131624.

[19] Molla AddisuMossie,Estifanos AbejeSharew,Tewodros GeraWorkineh & Yechale AmogneAlemu. (2025). Hybrid Modified Particle Swarm Optimization and Adaptive Neuro‐Fuzzy Inference System for Electric Power Consumption Prediction. International Journal of Photoenergy,2025(1),4715427-4715427.